Journal of Solid State Chemistry **153,** 336–341 (2000)
doi:10.1006/jssc.2000.8779, available online at http://www.idealibrary.com on IDEAL®

Phase Equilibrium in the System *Ln*–Mn–O

I. *Ln* = La at 1100°C

Kenzo Kitayama[1]

Department of Applied Chemistry and Biotechnology, Faculty of Engineering, Niigata Institute of Technology, Fujihashi, Kashiwazaki, Niigata 945-1195, Japan

Received February 4, 2000; in revised form May 10, 2000; accepted May 18, 2000; published online July 11, 2000

Phase equilibrium was established in the system La–Mn–O at 1100°C by changing the oxygen partial pressure from 0 to 15.00 in-log (P_{O_2}/atm). A phase diagram at 1100°C in presented for the system La_2O_3–MnO–MnO_2. Under the experimental conditions, La_2O_3, MnO, Mn_3O_4, and $LaMnO_3$ phases are present at 1100°C. La_2MnO_4, Mn_2O_3, and MnO_2 are not stable. Wide ranges of nonstoichiometry were found is the $LaMnO_3$ phase. x ranges from −0.050 at log $P_{O_2} = -13.05$ to 0.18 at log $P_{O_2} = 0$ in the form of $LaMnO_{3+x}$. The nonstoichiometry is represented with the equation, $N_O/N_{LaMnO_3} = 1.94\times10^{-4}(\log P_{O_2})^3 + 5.24\times10^{-3}(\log P_{O_2})^2 + 5.24\times10^{-2}(\log P_{O_2}) + 0.179$, and activities of the components in the solid solutions are calculated using this equation. $LaMnO_3$ seems to have a range of compositions from La_2O_3-rich to poor. Also MnO has a small nonstoichiometry at the oxygen-rich side. Lattice constants of $LaMnO_3$ were determined at different oxygen partial pressures. The crystal form of $LaMnO_3$ seems to change from orthorhombic to hexagonal as the oxygen partial pressure becomes higher. The standard Gibbs energy changes of the reactions in the phase diagram presented were calculated. © 2000 Academic Press

Key Words: **phase equilibrium; thermogravimetry; lanthanum–manganese oxide; standard Gibbs energy of reaction.**

Many reports have been published about magnetic, electronic, and crystallographic properties of $LaMnO_3$ (1,2). The magnetic order, moments, and ordering temperatures for $La_{1-t}MnO_{3+\delta}$ depend strongly on its nonstoichiometry (3).

According to a recent investigation of the stability of lanthanum manganite, $LaMnO_3$, in a reducing atmosphere between 350 and 600°C, two phases with a defective perovskite structure, $LaMnO_{2.875}$ and $LaMnO_{2.75}$, were stable (3). Kamata *et al.*, (4) used the thermogravimetric method at 1200°C to investigate the formation of $LaMnO_3$ in gas streams with gradually decreasing oxygen partial pressure and the perovskite phase $LaMnO_{3\pm\lambda}$ was revealed to have nonstoichiometry ranging from 2.947 to 3.079 under oxygen partial pressures below log (P_{O_2}/atm) = 0 at 1200°C. Nakamura *et al.* (5) also reported on the stability of $LaMnO_3$ based on isotherm reduction at 1000°C and they reported that the stability limit of the perovskite phases expressed in terms of $-\log(P_{O_2}/\text{bar})$ for $LaMnO_3$ is 15.05. Solid state equilibrium relations were studied in the region of the La–Mn–O system bounded by $LaMnO_3$, MnO, and La_2O_3. In the temperature range 900–1380°C the defective perovskite $LaMnO_{3-\lambda}$ coexists directly in equilibrium with lanthunum oxide and manganous oxide (6). Van Roosmalen *et al.* (7) presented the pseudobinary La_2O_3–Mn_2O_3 phase diagram in air and concluded that the perovskite-type $LaMnO_{3+\delta}$ solid solution can be formed with excess La as well as with excess Mn.

As described above, the detailed phase equilibrium of the La–Mn–O system at high temperatures was still not determined under controlled oxygen partial pressure.

Considering the above circumstances, the objectives of the present study are (1) to establish a detailed phase diagram for the system La–Mn–O at 1100°C as a function of the oxygen partial pressure and (2) to determine the thermochemical properties on the basis of the phase equilibrium.

EXPERIMENTAL

Analytical grade La_2O_3 (99.9%) and MnO (99.9%) were used as starting materials. MnO was dried by heating at 110°C in air. La_2O_3 was also dried at 1100°C. Mixtures with desired La_2O_3/MnO ratios were prepared by mixing throughly in an agate mortar and then were calcined several times during the intermediate mixing and treated by the procedures described previously (8).

The thermogravimetric method was mainly adopted in the present experiment, changing the oxygen partial pressure by passing a gas or mixed gases in the furnace. Mixed gases of CO_2 and H_2 and of CO_2 and O_2 were used to obtain the oxygen partial pressures in the present experiment.

[1]Fax: 0257-22-8142. E-mail: kitayama@acb.niit.ac.jp.

0022-4596/00 $35.00

The apparatus and procedures for controlling the oxygen partial pressure and keeping a constant temperature, the method of thermogravimetry, and the criterion for the establishment of equilibrium were the same as those described in the previous paper (9). The method of establishment of equilibrium is as follows: to ensure equilibrium, the equilibrium oxygen partial pressure of each sample was established from both sides of the reaction, that is to say, from low oxygen partial pressures to high oxygen partial pressures and vice versa. The balance, furnace, and gas mixer are schematically shown in Ref. (8). The furnace, which has a mullite tube wound with Pt 60%–Rh 40% alloy wire as heating element, is used vertically. Mixed gases, which make the desired oxygen partial pressures, pass from the bottom of the furnace to the top.

The identification of phases and the determination of lattice constants were performed using a Rigaku X-ray diffractometer Rint 2500 type apparatus employing Ni-filtered Cu$K\alpha$ radiation. A standard specimen of silicon was used to calibrate 2θ.

RESULTS AND DISCUSSIONS

(*1*) *Phase Equilibrium*

(*a*) *Mn–O system.* In the Mn–O system there have been known four oxides, MnO, Mn_3O_4, Mn_2O_3, and MnO_2. Under the present experimental conditions the system was reinvestigated, and in Fig. 1 the relationship between the oxygen partial pressure, $-\log(P_{O_2}/\text{atm})$, and the composition, O/Mn mol ratio, is shown. As shown in Fig. 1, the oxygen partial pressure in equilibrium with MnO and Mn_3O_4 is -5.40 ± 0.05 in $\log(P_{O_2}/\text{atm})$ and Mn_3O_4 is stoichiometric in the $-\log(P_{O_2}/\text{atm})$ range at least from 0 to 5.40. On the other hand, MnO has a slight non-stoichiometric composition at the oxygen-rich side. The O/Mn mol ratio is 1.0186 at -5.40 in $\log(P_{O_2}/\text{atm})$ and an equation, $N_O/N_{MnO} = 9.83 \times 10^{-4} (\log P_{O_2})^2 + 1.914 \times 10^{-2} (\log P_{O_2}) + 0.0933$, was obtained for the MnO solid solution in the oxygen partial pressure range from -10.00 to -5.40 using the least-squares method. Here, N_O and N_{MnO} are the mole fractions of oxygen and MnO in the solid solution. In Fig. 2 the relationship between x in MnO_x and $\log(P_{O_2}/\text{atm})$ is shown and x in MnO_x is represented by an equation, $x = 2.151 \times 10^{-4} (\log P_{O_2})^3 + 5.785 \times 10^{-3} (\log P_{O_2})^2 - 5.361 \times 10^{-2} (\log P_{O_2}) + 1.173$ ($\log P_{O_2}/\text{atm}$) (-5.40 to -10.00).

It was confirmed that MnO and Mn_3O_4 are stable under the present experimental conditions. The higher oxides, Mn_2O_3 and MnO_2, are not stable. This fact is also pointed out by van Roosmalen *et al.* (7), who presented the pseudobinary La_2O_3–Mn_2O_3 phase diagram in air (Fig. 6

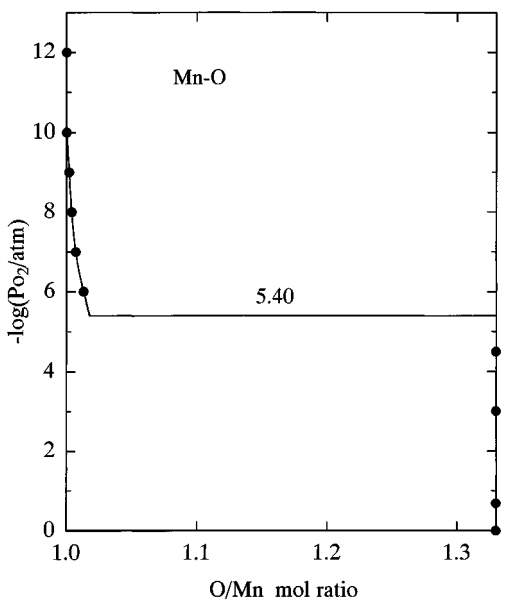

FIG. 1. Relationship between the oxygen partial pressure, log (P_{O_2}/atm), and the O/Mn mole ratio.

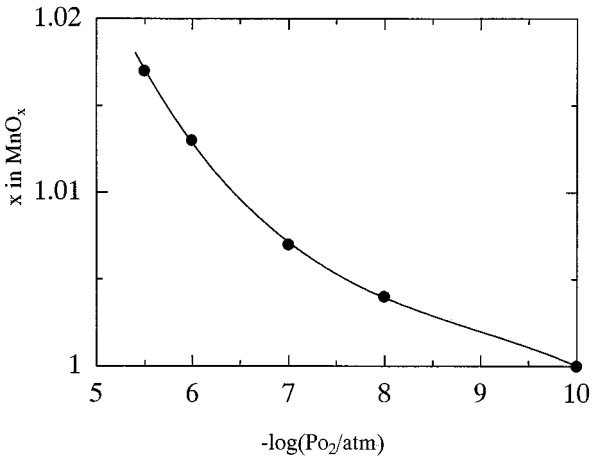

FIG. 2. Relationship between the oxygen partial pressure, log (P_{O_2}/atm), and x of the composition of MnO_x.

TABLE 1
Compositions, Symbols, Stability Ranges in Oxygen Partial Pressures, and Activities of Components in Solid Solutions

Component	Compositions	Symbols	$-\log(P_{O_2}/\text{atm})$	$\log a_i$
MnO	$MnO_{1.00}$	A_1	15.00–10.00	0
	$MnO_{1.02}$	A_2	5.40	-0.0137
$LaMnO_3$	$LaMnO_{2.95}$	B_1	13.05	0
	$LaMnO_{3.05}$	B_2	5.40	0.0542
	$LaMnO_{3.11}$	B_3[a]	0	—
	$LaMnO_{3.18}$	B_4[b]	0	6.72×10^{-3}

[a]Coexisting with Mn_3O_4. [b]Coexisting with La_2O_3.

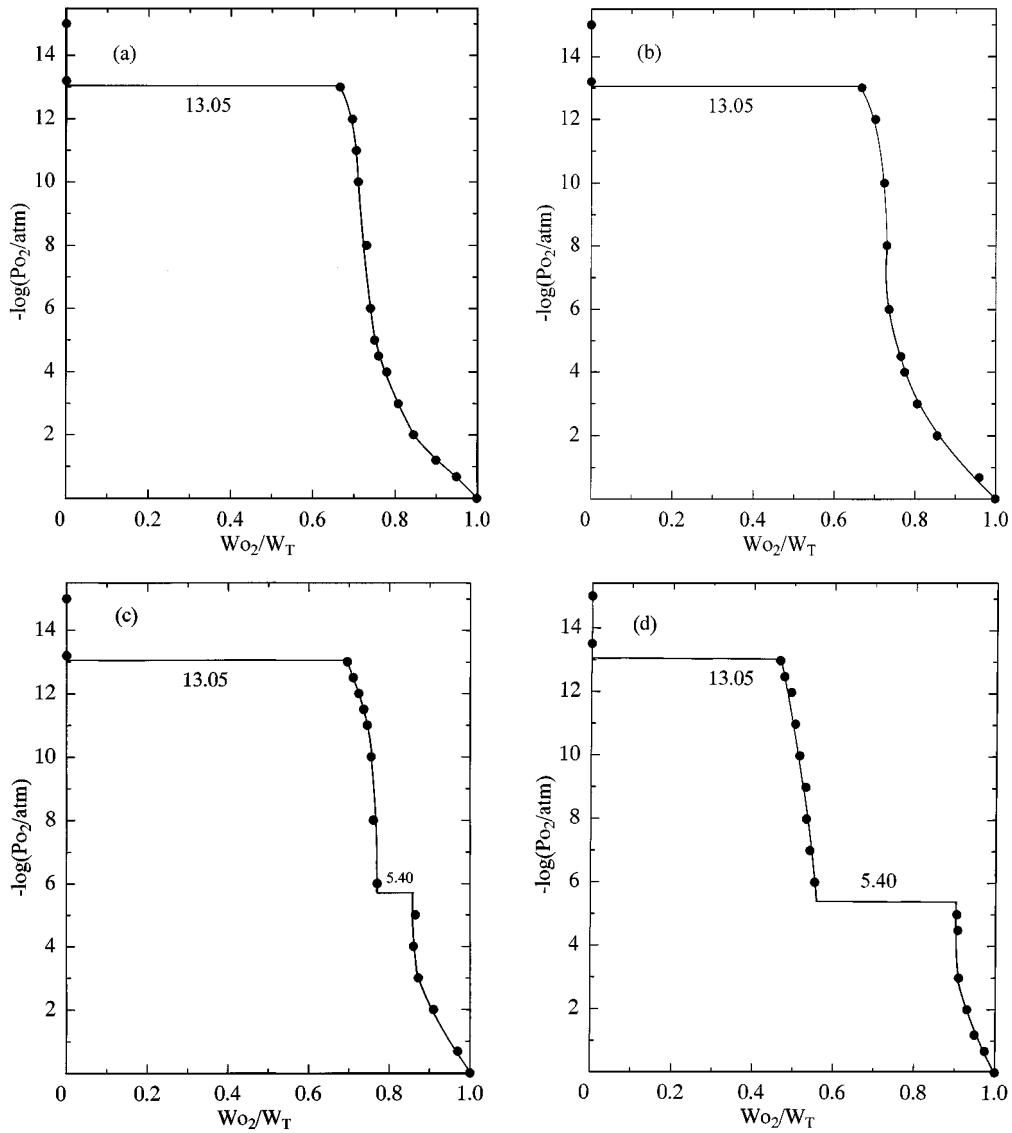

FIG. 3. Relationship between the oxygen partial pressure, log (P_{O_2}/atm), and the weight change of the samples, W_{O_2}/W_T. (a) La_2O_3/MnO = 5/5, (b) La_2O_3/MnO = 4/6, (c) La_2O_3/MnO = 3/7, and (d) La_2O_3/MnO = 2/8.

in Ref. (7)) and showed that below about 1150 K Mn_2O_3 is stable but at about 1150–1450 K t-Mn_3O_4 is stable.

Hahn and Muan (10) presented a general equation, log (P_{O_2}/atm) = 13.31 − 26,000/T, for the Mn_3O_4–MnO equilibrium. log P_{O_2} = −5.62 is obtained from this equation at 1100°C. This value is in fairly good agreement with the present value, −5.40.

The compositions, symbols, stability ranges of the solid solution in the oxygen partial pressures, and activities of components in the solid solution are tabulated in Table 1 together with activities of the components in the other solid solutions, which are necessary to calculate the equilibrium constant. The method for the calculation using the Gibbs–Duhem equation was described in a previous paper (9).

(*b*) *La_2O_3–MnO–MnO_2 system.* In this system the thermogravimetric method was adopted, too. Five samples with La_2O_3/MnO mole ratios of 6/4, 5/5, 4/6, 3/7, and 2/8 were prepared for use in thermogravimetry. In Fig. 3 the relationships between the oxygen partial pressure, −log (P_{O_2}/atm), on the ordinate and the weight changes, W_{O_2}/W_T, on the abscissa are shown for four representative samples, 5/5 (Fig. 3a), 4/6 (Fig. 3b), 3/7 (Fig. 3c), and 2/8 (Fig. 3d). Here, W_{O_2} is the weight increase of the samples from the reference weight at log (P_{O_2}/atm) = −15.00, at which La_2O_3 and MnO are

TABLE 2
Identification of Phase

Sample		$-\log (P_{O_2}/\text{atm})$	Time/h	Phases
La_2O_3	MnO			
		13.50	8	La_2O_3 + MnO
		12.80	8	La_2O_3 + $LaMnO_3$
		6.50	23	La_2O_3 + $LaMnO_3$
		5.00	14	La_2O_3 + $LaMnO_3$
		3.00	14.5	La_2O_3 + $LaMnO_3$
		0.68	15.5	La_2O_3 + $LaMnO_3$
0.40	0.60	13.50	8	La_2O_3 + MnO
		12.80	8	La_2O_3 + $LaMnO_3$
		6.50	23	La_2O_3 + $LaMnO_3$
		5.00	14	La_2O_3 + $LaMnO_3$
		3.00	14.5	La_2O_3 + $LaMnO_3$
		0.68	15.5	La_2O_3 + $LaMnO_3$
0.30	0.70	13.50	8	La_2O_3 + MnO
		12.80	8	$LaMnO_3$ + MnO
		6.50	23	$LaMnO_3$ + MnO
		5.00	14	$LaMnO_3$ + Mn_3O_4
		3.00	14.5	$LaMnO_3$ + Mn_3O_4
		0.68	15.5	$LaMnO_3$ + Mn_3O_4
0.20	0.80	13.50	8	La_2O_3 + MnO
		12.80	8	La_2O_3 + MnO
		6.50	23	$LaMnO_3$ + MnO
		5.00	14	$LaMnO_3$ + Mn_3O_4
		3.00	14.5	$LaMnO_3$ + Mn_3O_4
		0.68	15.5	$LaMnO_3$ + Mn_3O_4
0.00	1.00	12.80	8	MnO
		6.50	23	MnO
		5.00	14	Mn_3O_4
		0.68	15.5	Mn_3O_4

stable, and W_T is the total weight gain from the reference state to the weight at 1 atm of O_2, at which La_2O_3 and $LaMnO_3$ or $LaMnO_3$ and Mn_3O_4 are stable depending on the total composition of the samples. Weight breaks are found at 13.05 and 5.40 in $-\log (P_{O_2}/\text{atm})$. These values correspond to the oxygen partial pressure in equilibrium with three solid phases, $La_2O_3 + LaMnO_3 + MnO$ and $LaMnO_3 + MnO + Mn_3O_4$, respectively. The value -5.40 in $\log P_{O_2}$ corresponds to the value in equilibrium with MnO and Mn_3O_4 described above.

In Table 2 results of the identification of phases are shown in the Mn–O and La–Mn–O systems. About 500-mg samples for the identification of phases were made by the quenching method. Four phases, La_2O_3, MnO, Mn_3O_4, and $LaMnO_3$, are stable under the experimental conditions. Mn_2O_3 and MnO_2 are not stable. But Van Roosmalen *et al.* (7) pointed out the stability of ($P + Mn_2O_3$) are below $\sim$ 1120°C (Fig. 6 in Ref. (7)).

Based on the above results of thermogravimetry and the identifications of phases, a phase diagram was drawn and is shown in Fig. 4 for the La_2O_3–MnO–MnO_2 system, although MnO_2 is not stable under the experimental conditions. The numerical values in three solid fields in Fig. 4 are the two values in $-\log P_{O_2}$ in equilibrium with three solid phases described above. Numbers on the lines in the two phase regions are also the oxygen partial pressures in $-\log (P_{O_2}/\text{atm})$. The nonstoichiometry of MnO is ascertained by the results of thermogravimetry of other two samples, Figs. 3c and 3d. This is represented by slight changes of composition in the range of the oxygen partial pressure from 13.05 to 5.40 in $-\log P_{O_2}$.

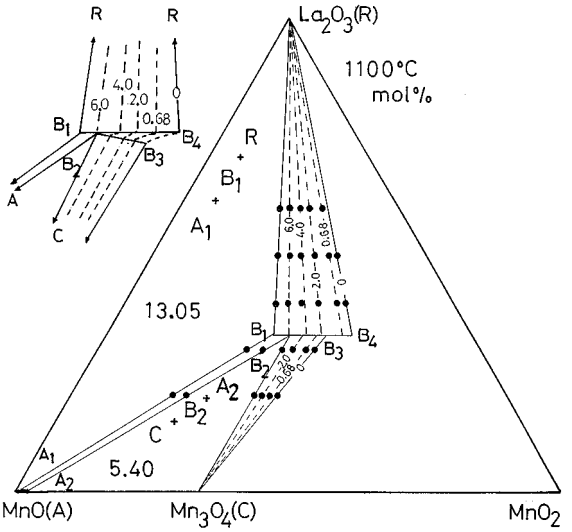

FIG. 4. Phase equilibrium in the La_2O_3–MnO–MnO_2 system at 1100°C. Numerical values in the three phase regions are the oxygen partial pressures in $-\log (P_{O_2}/\text{atm})$ in equilibrium with three solid phases which are shown in the regions. Abbreviations are the same as those in Table 1. A tentative detailed figure of $LaMnO_3$ solid solution part is shown at upper left side exaggeratedly.

$LaMnO_3$ has a large nonstoichiometric composition in the range from -13.05 to 0 in $\log P_{O_2}$. Besides, there are

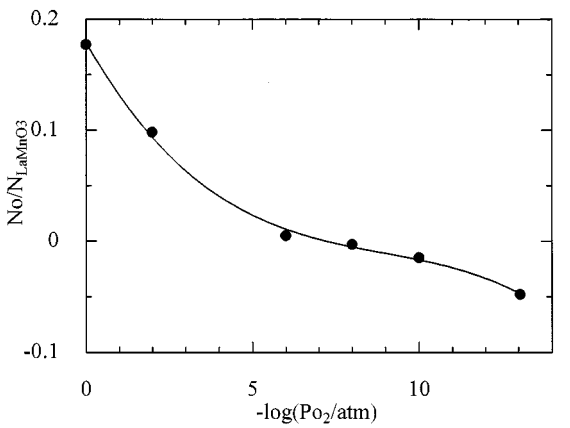

FIG. 5. Relationship between the oxygen partial pressure, $-\log (P_{O_2}/\text{atm})$, and the composition of $LaMnO_3$ solid solution, N_O/N_{LaMnO_3}.

TABLE 3
***d*-Spacing of Quenching Samples of $La_2O_3/MnO=0.4/0.6$ at Various Oxygen Partial Pressures**

$LaMnO_3$[a]	$-\log (P_{O_2}/atm)$				$LaMnO_{3.15}$[b]
	12.80	6.50	3.00	0.68 (air)	
3.983	3.992	3.992	3.931	3.904	3.86
3.844	3.855	3.855	3.889	—	—
3.537	3.545	3.545	3.511	—	—
2.870	2.878	2.869	2.795	—	—
2.768	2.774	2.774	2.765	2.758	2.75
2.689	2.696	2.688	2.631	—	2.72
2.300	2.305	2.299	2.269	—	2.34
2.245	2.250	2.250	2.255	2.252	2.24
2.155	2.159	2.159	—	—	2.22
1.993	1.994	1.992	—	—	—
1.923	1.926	1.926	1.944	1.951	1.937
1.769	1.771	1.770	—	—	1.797
1.761	1.764	—	—	—	—
1.757	1.754	—	—	—	—
1.732	1.734	1.735	1.740	1.743	1.741
1.712	—	—	1.722	1.700	1.727
1.637	1.643	1.635	—	—	—
—	—	—	1.607	—	—
1.598	1.599	1.599	1.596	1.591	1.591
1.579	1.580	1.581	—	—	1.585
1.574	1.575	—	—	—	1.570
1.479	1.480	1.478	1.459	—	1.492
1.411	1.413	—	1.398	—	—
1.384	1.385	1.385	1.382	1.383	—
—	—	—	—	1.378	1.379
1.300	1.307	1.307	—	1.302	1.294

Note. *d*-values of La_2O_3 are omitted.
[a]JCPDS Card No. 35-1353, orthorhombic. [b]JCPDS Card No. 32-484, hexagonal.

oxygen partial pressures in equilibrium with a composition of $LaMnO_3$ solid solution at the La_2O_3-rich side and -poor side which do not cross at the same composition. It is guessed that this results from the width of $LaMnO_3$ composition toward the La_2O_3 side or Mn_3O_4. Van Roosmalen *et al.* (7) reported that the perovskite-type $LaMnO_{3+\delta}$ solid solution can be formed with excess La as well as with excess Mn. A tentative detailed figure of the $LaMnO_3$ part is drawn in the upper left part of Fig. 4 as an exaggeration although its width cannot be detected by present experimental techniques. The curved lines of $\log P_{O_2}$ in the figure result from the phase rule; that is, one phase area has two degrees of freedom. So the oxygen partial pressure lines in one phase region, the $LaMnO_3$ phase, might be curves.

In Fig. 5, using the oxygen partial pressure in equilibrium with the composition of $LaMnO_3$ solid solution data for the La_2O_3-rich side, an equation was obtained as follows: $N_O/N_{LaMnO_3} = 1.96\times10^{-4}(\log P_{O_2})^3 + 5.24\times10^{-3}(\log P_{O_2})^2 + 5.25\times10^{-2}(\log P_{O_2}) + 0.179$. The phases $La_8Mn_8O_{23}$ and $La_4Mn_4O_{11}$ were found in carbon monoxide at lower temperatures of 450°C and 520°C by Abbattista *et al.* (11). But as shown in Fig. 4, more such oxygen defects are found and discrete phases are not stable under the present experimental conditions.

In Table 3 *d*-values for four samples of $La_2O_3/MnO = 0.4/0.6$, which are quenched in four different oxygen partial pressures, are shown together with those of $LaMnO_3$ (JCPDS Card No. 35-1353, orthorhombic) and $LaMnO_{3.15}$ (JCPDS Card No. 32-484, hexagonal). This seems to show that the orthorhombic type oxygen-poor transforms to hexagonal oxygen-rich (nonstoichiometric composition) as the oxygen partial pressures change from -12.80 to high -0.68 in $\log (P_{O_2}/atm)$. Also, lattice constants of various quenched samples with La_2O_3 are shown in Table 4 together with previous values. These present values are in fairly good agreement with previous values. The lattice constants for a sample made in air ($\log P_{O_2} = -0.68$) fit better to the hexagonal than the orthorhombic type.

(*2*) *The Standard Gibbs Energy Change of Reaction*

On the basis of the established phase diagram, standard Gibbs energy changes of reactions, which appear in the

TABLE 4
Lattice Constants of Quenched $LaMnO_3$ Coexisting with La_2O_3

$-\log (P_{O_2}/atm)$	*a*/Å	*b*/Å	*c*/Å	*V*/Å^3	Source
12.80	5.534 ± 0.006	5.736 ± 0.008	7.692 ± 0.011	244.1 ± 0.5	This work
6.50	5.534 ± 0.006	5.709 ± 0.011	7.698 ± 0.015	243.2 ± 0.7	This work
	5.536	5.726	7.697		33–713[a]
	5.537	5.741	7.694		35–1353[a]
0.68	5.503 ± 0.006	—	13.57 ± 0.12	356 ± 3	This work[b]
	5.523	—	13.324		32–484[a]

[a]JCPDS Card No.
[b]As hexagonal.

TABLE 5
Standard Gibbs Energy Changes of Reaction at 1100°C

Reaction	$-\log P_{O_2}$ (atm)	$-\Delta G^\circ$ (kJ/mol)
(1) $3MnO + 1/2O_2 \rightarrow Mn_3O_4$	5.40 ± 0.05	72.1 ± 0.3
	5.62	73.9[a]
		60.4[b]
		50.9[c]
(2) $1/2La_2O_3 + MnO + 1/4O_2 \rightarrow LaMnO_3$	13.05 ± 0.03	85.8 ± 0.3

[a]Ref. (10).
[b]Ref. (12).
[c]Ref. (13).

phase diagram and are shown in Table 5, are determined with an equation, $\Delta G^\circ = -RT \ln K$. Here, R is the gas constant, T the absolute temperature, and K the equilibrium constant of the reaction.The standard states of the activities of components in the solid solutions can be arbitrarily chosen for each solid solution and are indicated as $\log a_i = 0$ in Table 1.

The standard Gibbs energy change for reaction [1] is -72.1 ± 0.3 kJ/mol. Assuming that the activity of MnO of the composition (A_2) is unity, this value is -75.0 ± 0.3 kJ/mol. On account of a small solid solution range, the difference is not great.

Calculations made with previous data from Refs. (12) and (13), $-60.4\ \text{kJ mol}^{-1}$ and $50.9\ \text{kJ mol}^{-1}$, are obtained, respectively. The reason for these large differences is not known now.

ACKNOWLEDGMENTS

The author thanks Dr. Masanobu Kusakabe for help in technical support for the X-ray program.

REFERENCES

1. J. B. Goodenough, *Prog. Solid State Chem.* **5,** 149 (1971).
2. C. N. R. Rao, *Annu. Rev. Phys. Chem.* **40,** 291 (1989).
3. B. C. Hauback, H. Fjellvag, and N. Sakai, *J. Solid State Chem.* **124,** 43 (1996).
4. K. Kamata, T. Nakajima, T. Hayashi, and T. Nakamura, *Mater. Res. Bull.* **13,** 49 (1978).
5. T. Nakamura, G. Petzow, and L. J. Gauckler, *Mater. Res. Bull.* **14,** 649 (1979).
6. M. Lucco Borlera and F. Abbattista, *J. Less-Common Metals* **92,** 55 (1983).
7. J. A. M. van Roosmalen, P. van Vlaanderen, E. H. P. Cordfunke, W. L. Ijdo, and D. J. W. Ijdo, *J. Solid State Chem.* **114,** 516 (1995).
8. K. Kitayama, *J. Solid State Chem.* **137,** 255 (1998).
9. K. Kitayama, K. Nojiri, T. Sugihara, and T. Katsura, *J. Solid State Chem.* **56,** 1 (1985).
10. W. C. Hahn, Jr., and A. Muan, *Am. J. Sci.* **258,** 66 (1960).
11. F. Abbattista and M. Lucco Borlera, *Ceram. Int.* **7(4)** 137 (1981).
12. R. A. Robic, R.S. Hemingway, and J. R. Fisher, "Thermodynamic Properties of Minerals and Related Substances at 298.15 K and 1 Bar (10^5 Pascals) Pressure and at Higher Temperatures," Geological Survey Bulletin 1452. United States Government Printing Office, Washington, 1978.
13. J. F. Elliott and M. Gleiser, "Thermochemistry for Steelmaking," Vol. 1. Addison-Wesley, Reading, MA, 1960.